Effect of Humidity on the Supramolecular Structure of Cotton, Studied by Quantitative Spin Probing

S. Frantz, G. A. Hübner,[†] O. Wendland,[‡] and E. Roduner*

Institute of Physical Chemistry, University of Stuttgart, Pfaffenwaldring 55, D-70569 Stuttgart, Germany

C. Mariani and M. F. Ottaviani

Institute of Chemical Sciences, University of Urbino, Piazza Rinascimento 6, 61029 Urbino, Italy

S. N. Batchelor*

Unilever Research Port Sunlight, Quarry Road East, Bebington, Wirral CH63 3JW, United Kingdom

Received: February 15, 2005; In Final Form: April 11, 2005

The effect of water content on the physicochemical properties of the amorphous regions in cotton were investigated by measuring the electron paramagnetic resonance (EPR) of TEMPOL nitroxide radicals, deposited in cotton at different loadings, as a function of the relative humidity (RH) and temperature. Three different components contribute differently to the experimental EPR spectra, corresponding to (a) mobile radicals absorbed in the bulk amorphous region, (b) slow moving radicals adsorbed on the crystallite surfaces in cotton, and (c) aggregated radicals. These components were analyzed by means of computer-aided simulations of the line shapes and simplified line width methods. Polarity and mobility parameters were extracted from the analysis of the spectra. For all loadings and temperatures, the polarity suddenly dropped when the water content fell below ∼3 wt %, i.e., when water was removed from the bulk amorphous regions. At the lowest loading (2×10^{-5} mol kg^{-1}), the spectra were independent of the RH, and only mobile radicals were observed. At intermediate loading (10^{-4}−10^{-3} mol kg^{-1}) both mobile (fast) and adsorbed (slow) moving radicals were present, the fraction of which depended on the RH. The mobility of the adsorbed and mobile radical signals was smaller at higher loadings, indicating microdomains of different character. The temperature dependence of the rotational correlation times provided the activation energies, which were much lower than in liquids. An equilibrium exists between the mobile and the adsorbed radicals. The temperature dependence of the equilibrium constant, *K*, gave the enthalpy and the entropy of the adsorption process. At low RH, the enthalpy and the entropy values indicated a simple adsorption process. At 10^{-3} mol kg^{-1}, the values were independent of the RH, but at low loadings the values increased with the increase in the RH, which suggested a displacement of adsorbed water by the radicals at high water content. At loadings above 10^{-3} mol kg^{-1}, signals from radicals strongly interacting via spin exchange were observed, which are assigned to aggregated radicals; simulation of the spectra gave an activation energy of 13 kJ mol^{-1} for the spin exchange process. These effects are rationalized on the basis of microdomains of different character within cotton, reflecting the variation in pore sizes (0.5−8 nm) and the relaxation behavior of the cellulose chains.

1. Introduction

Cotton has been used by mankind for at least 7000 years[1] and cultivated for more than 4500 years.[2] Today, the world production of cotton is approximately 20 million tons per annum,[3] mainly for clothing, paper, and medical uses. It is a remarkably pure fiber, constructed from polysaccharide chains arranged into amorphous and crystalline regions. The amorphous regions are slit pores of a few nanometers in width situated between the crystallites and are readily accessible to external agents.[4,5] Hence, cotton represents the oldest and most commonly used nanoporous material. However, relatively little is known about the structure of the amorphous phase or the behavior of molecules within the nanopores.

A striking and extremely useful feature of cotton is its ability to absorb large quantities of liquids, particularly water.[5] In the range 0−3 wt %, the water is adsorbed onto the crystallite surfaces; then as the level increases, it starts to occupy the amorphous region in a bulk absorption mechanism.[6,7] Both of these types of water are nonfreezing, i.e., strongly interacting with the cellulose. Above approximately 10%, the water then fills the space between the growth ring of the fiber. In the 0−10% range, the equilibrium water content is controlled by air humidity;[8] for example, between 5% and 70% relative humidity (RH) the water content increases from 1.5 to 7.8 wt % at 303 K. It is well-known that the water changes the mechanical properties of the fiber[9] and is thought to affect the pore structure.[10] Information on the detailed changes in the nanostructure, the polysaccharide chain motion, and the behavior

* Authors to whom correspondence should be addressed. E-mail: e.roduner@ipc.uni-stuttgart.de; Stephen.Batchelor@unilever.com.

[†] Present address: Ingenieurgesellschaft Auto und Verkehr, Nordhoffstrasse 5, 38518 Gifhorn, Germany.

[‡] Present address: Boehringer-Anschrift, Boehringer Ingelheim Pharma GmbH & Co., KG Binger Strasse 173, 55216 Ingelheim am Rhein, Germany.

10.1021/jp050791x CCC: $30.25
Published on Web 05/18/2005

TABLE 1: Saturated Salt Solutions and Water Content of Cotton[7]

	% RH	*A*	*B*
NaOH	6	5.84	0.0141
LiCl	11	7.81	0.0186
$MgCl_2$	33	12.81	0.0287
NaCl	75	24.94	0.0535

of other molecules within the nanopores would be useful in understanding mechanical processes such as the wrinkling and ironing of cotton garments and in understanding the effect of humidity on the chemistry of adsorbed species such as dyes.[11]

Electron paramagnetic resonance (EPR) spectroscopy studies of nitroxide probe radicals in dry cotton have given valuable insight into the amorphous region.[12,13] Depending on the loading, the radicals exist in three states within the amorphous pores, either readily mobile in the amorphous region (equivalent to absorbed water), adsorbed onto the surface of crystallites, or aggregated together. Analysis of the spectra allowed quantification of the equilibrium between mobile and adsorbed radicals, the aggregation limit, and gave the microviscosity of the amorphous region. It also showed the existence of microdomains of different character within cotton leading to different behavior of the radicals with loading. As the experiments were only conducted under normal laboratory humidities ($\sim$ 60−70% RH), little information is available on the effect of water content on the amorphous nanopores of the fiber. The aim of the current work is to study this effect, and spin probe experiments on cotton are reported with loadings from 2.0×10^{-5} to 1.0×10^{-2} mol kg^{-1} at relative humidities between 6% and 75% over the temperature range of 293 to 323 K.

2. Experimental Section

Bleached and unmercerized cotton sheeting was obtained from a commercial supplier (Phoenix Calico) and used as received. The cotton was cut into 10×150 mm^2 strips and then placed into a solution of a known concentration of TEMPOL (4-hydroxy-2,2,6,6-tetramethyl-1-piperidinyloxy) (Merck) in ethanol (Merck). The cloth was withdrawn after 30 s, the excess solvent was removed, and then the cloth was dried in air at 40 °C for 30 min. This delivered a known weight (±20%) of TEMPOL into the cotton, calculated on the basis of the amount of ethanol absorbed by wet cotton and allowed the loading in moles per kilogram cotton to be calculated.

The dried cotton was suspended above various saturated salt solutions in a sealed quartz sample tube 5 mm in diameter. The salt solutions used are given in Table 1, alongside the relative humidity in the air that they create.[14] These humidity values are constant between 293 and 323 K, and measurements were limited to this temperature range. For these humidity and temperature ranges, the cotton water content may be accurately predicted from literature data[8] using the linear equation

$$W = A - BT \quad (1)$$

where W is the quantity of water in grams per 100 g of dry cotton, T is the temperature in Kelvin, and the values for A and B are given in Table 1. As expected, the water content increases with increasing humidity.

EPR spectra were recorded using a Bruker EMX X-band EPR spectrometer. Samples were allowed to equilibrate for at least 16 h at room temperature before measuring. The temperature was measured using a K-type thermocouple placed in the nitrogen flow at the bottom of the cavity. The temperature accuracy was within ±1 K. To avoid any spectral distortion, the incident microwave power was kept at 2 mW, well below saturation, and the modulation amplitude was 1 G. In general, a scan range of 200 or 300 G with a scan time of 11.2 min and a time constant of 328 ms was used. A total of 128 spectra were recorded, eight loadings (1.0×10^{-2}, 3.0×10^{-3}, 1.1×10^{-3}, 7.4×10^{-4}, 4.0×10^{-4}, 1.6×10^{-4}, 5.0×10^{-5}, and 2.0×10^{-5} mol kg^{-1}), each at four relative humidities of the ambient air in the sample tube (6%, 11%, 33%, and 75%) and four temperatures (293, 303, 313, and 323 K).

3. Results

To follow the results, it is important to bear in mind the distinction between *absorbed* and *adsorbed* species. As discussed in the Introduction, within cotton species may be adsorbed onto the surface of the crystallites or absorbed into the bulk amorphous regions.

3.1. EPR Spectra. Typical EPR spectra are shown in Figure 1, and large variations with humidity, temperature, and loading are observed. For the lowest loading of 2.0×10^{-5} mol kg^{-1}, a three-line spectrum of freely tumbling radicals is observed at all humidities, which is characteristic of mobile radicals absorbed in the bulk amorphous pores (further denoted as the mobile fraction). As the loading increases to 1.6×10^{-4} mol kg^{-1}, the spectra become an admixture of a mobile spectrum and a powder spectrum, the latter indicating the presence of radicals adsorbed onto the crystallite surfaces (the adsorbed fraction). This change in spectra with loading is due to the presence of microdomains of different character within cotton;[13] the preferred microdomains (PMD) where only mobile radicals are observed are occupied first, then the more numerous domains where the adsorbed radicals can also be seen.

Notably the change from purely mobile to the mobile/adsorbed radicals is humidity-dependent. At 1.6×10^{-4} mol kg^{-1} and 6% RH, the radicals are predominately adsorbed, but as the humidity increases the adsorbed fraction steadily decreases until at 75% the radicals are predominately mobile. A similar pattern is observed at 1.1×10^{-3} mol kg^{-1}, except that here the adsorbed fraction is clearly larger, even at the higher humidities. Increasing the loading further to 1.0×10^{-2} mol kg^{-1} leads to spectra dominated by a single broad line for all humidities. The broad line represents radicals that are undergoing rapid spin exchange and has been assigned to aggregated radicals.[13] Increasing temperature leads to a higher fraction of mobile radicals at all loadings and all humidities.

Consequently, the fiber water content, controlled by humidity, can greatly change the behavior of radicals in the cotton nanopores, although the effects are strongly loading-dependent. At the lowest (2.0×10^{-5} mol kg^{-1}) and highest measured loadings (1.0×10^{-2} mol kg^{-1}), the changes with humidity are small, unlike the dramatic changes at the intermediate loadings (1.6×10^{-4}−1.1×10^{-3} mol kg^{-1}). To fully understand these effects required detailed quantification and interpretation of the spectra, which is given below.

3.2. Mobile Phase. *3.2.1. Micropolarity.* The isotropic hyperfine coupling constant, a_N, of the mobile nitroxide radicals may be easily measured directly from the spectra and provides an excellent measure of the micropolarity.[15] Within error, these values did not depend on loading or temperature but did show a change with humidity, Figure 2. Above 3.5 g water/100 g dry cotton (294 K), the coupling constant is 16.8 G, close to that in water (16.9 G), whereas below the 2.5 g water/100 g dry cotton level the coupling is 16.3 G, similar to that in ethylene glycol.[15] Thus, as water is removed from cotton, the polarity in all the microdomains drops rapidly between 2.5 and 3.5 g water/100 g cotton, and TEMPOL senses a less polar environment.

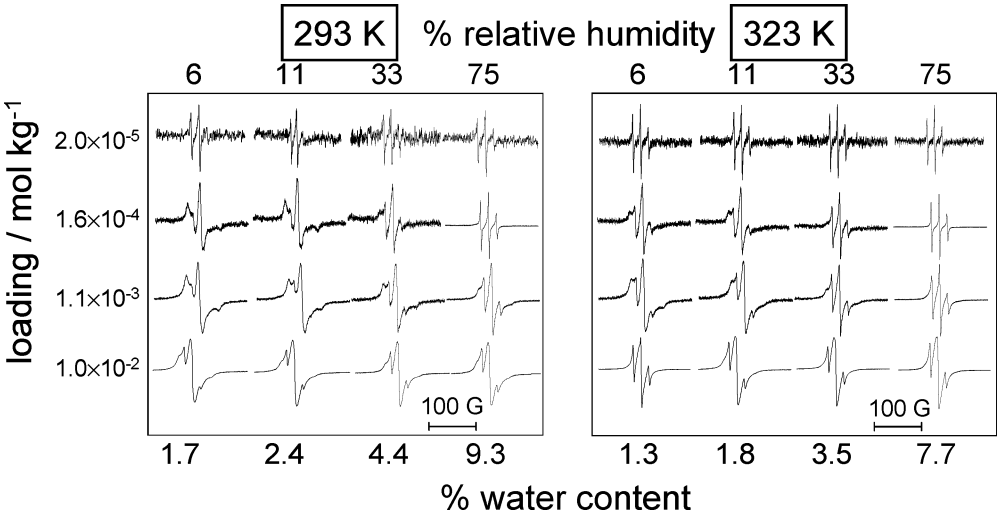

Figure 1. Influence of loading and relative humidity on the EPR spectrum of TEMPOL radicals in cotton.

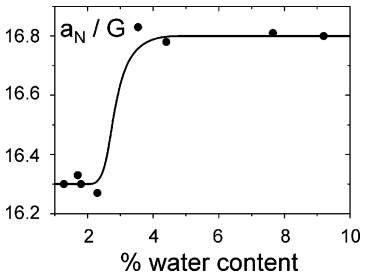

Figure 2. Variation of the isotropic nitrogen hyperfine coupling, a_N, constant with water content. Within experimental error, the behavior was independent of loading and temperature.

The onset of the polarity increase in Figure 2 is at approximately 3% water content, which is also the maximum amount of water[6,7,16] that can be adsorbed on the crystallite surfaces. At higher levels, the water starts to be within the bulk amorphous regions, like the mobile TEMPOL radicals. Thus the change in polarity of the mobile fraction of the TEMPOL radicals corresponds to the introduction of water into the bulk amorphous regions. Below 3% water content, the radicals feel a polyalcohol environment (ethylene glycol), which would be expected for an environment dominated by polysaccharide. It is surprising that the change in micropolarity is so rapid as addition of less than 0.5 g water/100 g dry cotton into the bulk amorphous regions causes the change. This points to the water and TEMPOL being clustered together rather than randomly distributed throughout the amorphous region. Studies of self-aggregation of dyes,[17] ketones,[18] and nitroxides[13] in cellulose/cotton all show aggregation occurring at loadings of 10^{-2} mol kg^{-1}. If the same limit applies for TEMPOL−water aggregation, then the micropolarity should rapidly increase when only 0.02 g water/100 g cotton is introduced into the bulk amorphous regions, in agreement with the results.

3.2.2. Rotational Motion and Microviscosity. To quantify the changes in the rotational motion of the mobile radicals, the spectra were simulated using the well-established method of Freed et al.,[19] which yields the isotropic rotational correlation time, τ, of the radical. Due to the complexity of the spectra, a simpler line width method was also used to obtain τ in many cases.[10] Simulation of the mobile fraction required the known g tensors of the radical ($g_x = 2.009$, $g_y = 2.006$, $g_z = 2.002$).[21] The components of the hyperfine tensor were set (with $a_{zz} =$ 36.5 G, the z-direction is perpendicular to the plane defined by the bond centers of the puckered six-ring structure of TEMPOL), as was the line width (0.45 G along the N−O axis), and then τ was obtained by fitting. A completely isotropic Brownian motion was assumed. Kuznetsov[21] correlated the heights of the single lines with the anisotropy of rotation for the fast rotation regime. If the first two lines are of equal height, then the rotation is isotropic. To a reasonable approximation, it is the case for our mobile species, Figure 1. The fact that the low field line is slightly less intense reveals that the rotation about the N−O axis is somewhat slower than for the other axes. Due to the oblate shape of the TEMPOL molecule, this is to some extent also the case in plain aqueous solutions. The effect may be enhanced for the mobile species in the pore of cotton, due to anisotropic interaction with the environment and to the increase of the apparent microviscosity in the pore.

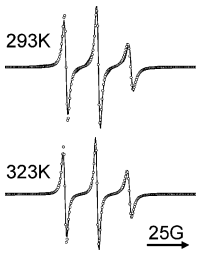

Figure 3. Spectra (full line) and simulations of the mobile TEMPOL radicals, at 1.6×10^{-4} mol kg^{-1}.

TABLE 2: Comparison between the Results Obtained by the Line Width Method and the Simulations for the Mobile Phases at the Highest Relative Humidity

		simulations		line width method	
loading (mol kg^{-1})	temperature (K)	τ (ns)	η (cP)	τ (ns)	η (cP)
1.6×10^{-4}	293	0.527	12.3	0.777	14.4
	303	0.481	11.6	0.714	14.7
	313	0.428	10.7	0.660	14.6
	323	0.391	10.0	0.613	14.3
2.0×10^{-5}	293	0.428	10.0	0.555	12.9
	303	0.382	9.2	0.618	14.9
	313	0.348	8.7	0.561	14.0
	323	0.318	8.2	0.525	13.5

At low loadings, good simulations were obtained as illustrated in Figure 3, and the fitted τ values are given in Table 2. The small temperature dependence could be fit well using an Arrhenius-type expression[22]

$$\tau = A \exp(-E_a/RT) \qquad (2)$$

where E_a is the activation energy for molecular reorientation.

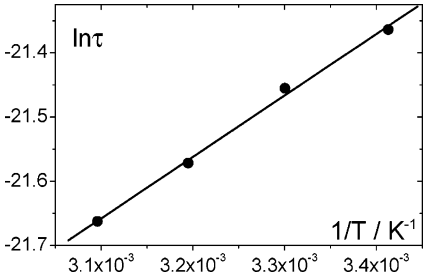

Figure 4. Arrhenius plot for the rotation correlation time at 1.6×10^{-4} mol kg^{-1} and 75% RH.

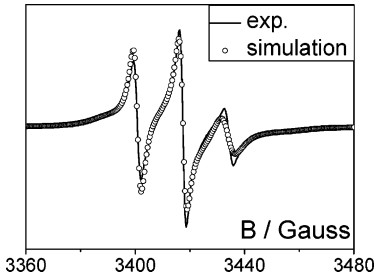

Figure 5. Spectrum and full simulation at 1.1×10^{-3} mol kg^{-1}, 75% RH, and 323 K. The ratio of mobile/adsorbed/aggregated radical was 100:20:3.

For both studied loadings, 1.6×10^{-4} (Figure 4) and 2.0×10^{-5} mol kg^{-1}, values of 8 kJ mol^{-1} were obtained for E_a.

Naturally, as the adsorbed fraction increases, the fits and reliability of the computed τ became worse. It was possible to simulate the overall spectrum at a loading of 1.1×10^{-3} mol kg^{-1} at 323 K (Figure 5). However, this is time-consuming and may induce errors because it requires the superposition of simulated mobile, aggregated, and adsorbed components. In this situation, a line width method was used to obtain τ, which involves measuring ΔH_0, the peak-to-peak line width of the central line in G and using the equation[24]

$$\tau/\mathrm{s} = 3.0 \times 10^{-10} \times \Delta H_0/\mathrm{G} \approx 3.0 \times 10^{-10} \times \Delta H_+/\mathrm{G} \quad (3)$$

As the low field line width ΔH_+ is almost identical to ΔH_0, it may be used instead. This further approximation has the great advantage that in the spectra ΔH_+ suffers much less distortion by the adsorbed and aggregated fractions than ΔH_0. This method was used to calculate τ for all spectra, and in places where the simulation method was also applied, good agreement was found, Table 2. In the low loading situation where only the mobile spectrum is observed, the simulation is more accurate than the line width method as it assess the full spectrum rather than just a small part of it. Thus the line width method does not pick up the small temperature dependence in τ.

Previous work has shown that the rotational and translational diffusion of radicals in cotton may both be rationalized using a simple liquid model for motion in the amorphous region.[12,13,24,25] Following this strategy, the τ values were converted into microviscosities, η, via the Debye formula, for detailed interpretation

$$\tau = \frac{4\pi r^3 \eta}{3k_B T} = \frac{4\pi r^3}{3k_B T}\eta_o \exp\left(\frac{E_a'}{RT}\right) \quad (4)$$

where k_B denotes the Boltzmann constant, T is the temperature in Kelvin, $r = 0.346$ nm is the radical's radius, calculated from increments,[26] and E_a' the activation energy for viscosity. This

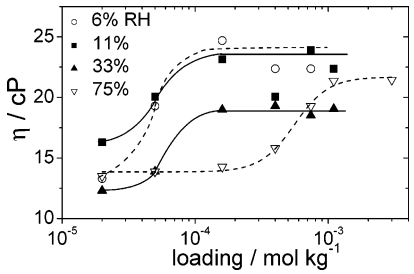

Figure 6. Change of microviscosity with loading at 323 K for all studied humidities. The lines are guides only and have no theoretical significance.

expression shows that the preexponential factor in eq 2 scales as $1/T$. However, it does not affect the linearity of the Arrhenius plots since the chosen temperature range is small. By comparison of $\mathrm{d}(\ln \tau)/\mathrm{d}T$ obtained from eq 2 and eq 4, the activation energy for viscosity can be expressed as $E_a' = E_a - RT$. This gives a value of about 5.5 ± 0.2 kJ mol^{-1} for the studied temperature range. It is lower than the activation energies found in liquids; for example, water and ethylene glycol have values of 15.6 and 25.9 kJ mol^{-1}, respectively.[14]

Prior spin probe work[13] showed a much stronger temperature dependence for the microviscosity. However, in this work the classical equations[23] used to extract τ also involved the heights of the three hyperfine lines. Since the central line is distorted by signals from the adsorbed and aggregated fraction, which vary with temperature, an anomalous temperature dependence is introduced.

The most reliable values for η are those at the highest temperature where the mobile fraction is greatest, and the values (obtained via the line width method) are shown in Figure 6. At all humidities, a sigmoidal behavior is observed. For 75% RH as the loading increases, the viscosity is almost constant at 14 cP up to 2×10^{-4} mol kg^{-1}, then inflects and rises to 22 cP by 10^{-3} mol kg^{-1}, and remains constant. At 33% RH, the behavior is similar with terminal values slightly smaller than for 75% RH and a shift of the inflection point to lower loadings. The two curves corresponding to the lowest humidities (6% and 11% RH) are almost identical to each other, the inflection point is further shifted to lower loadings, and the viscosities are slightly higher than those for the higher humidities. The microviscosity values obtained here are in reasonable agreement with those previously reported at laboratory humidity (60−70% RH) using spin probes and other independent methods, which gave a low loading value of 15−20 cP[13] and a high loading value of ∼30 cP.[6,12,13,24,25]

These effects provide strong evidence for the existence of microdomains of different character and behavior within cotton.[13] This concept is entirely reasonable considering the variation in the observed pore size in cotton, from 0.5 to 8 nm,[4,27] as molecules within the large and small pores would be expected to behave differently. In the simplest approximation, there are two microdomains, the PMDs, which are occupied first and hence observed at the lowest loadings, and the more numerous microdomains (NMDs) observed at higher loadings where they dominate the spectra. In the following, the NMDs are defined from Figure 6 as the domains occupied at greater than approximately 10^{-3} mol kg^{-1} that show little or no variation in their microviscosity over the humidity range measured. The PMDs are those occupied at lower loadings, which at 75% all have a microviscosity of 14 cP and most of which show a relatively strong humidity dependence.

The humidity dependence may be quantified by the inflection point in Figure 6, where the microviscosity starts to rise, and

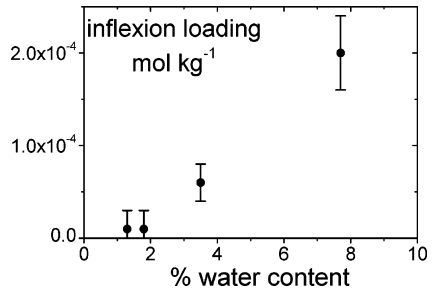

Figure 7. Dependence of the inflection loading on water content. The inflection loading is the point in Figure 6 when the microviscosity starts to rise.

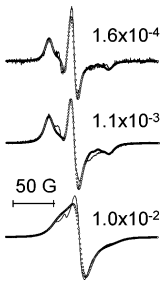

Figure 8. Spectra and simulations of the adsorbed phase, at 6% RH and 293 K. (Note that the minimum/maximum of the middle line in the simulation is often not identical to the experimental spectrum; this is due to the distortion of the middle line caused by the superposition of two phases).

TABLE 3: Results Obtained by Simulations of Adsorbed (1.6×10^{-4} and 1.1×10^{-3} mol kg^{-1}) and Aggregated (1.0×10^{-2} mol kg^{-1}) Phases at the Lowest Relative Humidity

loading (mol kg^{-1})	temperature (K)	τ (ns)	η (cP)	W_{ex} (10^7 s^{-1})
1.6×10^{-4}	293	10.0	235	
	303	8.91	215	
	313	8.32	207	
	323	7.41	190	
1.1×10^{-3}	295	17.8	418	5.62
	303	15.8	381	6.31
	313	14.1	351	7.94
	323	12.6	324	8.91
1.0×10^{-2}	295	17.8		24.0
	303	15.8		27.5
	313	14.1		32.4
	323	12.6		38.0

is, for example, 2×10^{-4} mol kg^{-1} at 75% RH. This is plotted in Figure 7 and is constant at 2×10^{-5} mol kg^{-1} below ~3% water content where only adsorbed water on the crystallite surface is present. Above ~3%, where water is absorbed in the bulk amorphous regions, it rises rapidly. At 75% RH, the amorphous regions are essentially saturated with water, so that at higher water contents little further changes in the inflection point would be expected. Consequently, for the majority of the PMDs the microviscosity shows a dependence on absorbed water, and this water gives them a lower viscosity than that of the NMDs. However, approximately 10% of the PMDs show no dependence and are the most "preferred" PMDs.

These observations cannot be assigned to large structural changes in cotton, as X-ray diffraction studies have shown little variation in the crystallinity with water content.[28] They therefore must be due to changes in the motion of the cellulose chains in the amorphous regions. For the NMDs, no humidity dependence on the microviscosity is observed, and this leads to the simple conclusion that for these domains the microviscosity is independent of water content in the measured range. Consequently, the motion of TEMPOL must be determined by the cellulose chains alone. Mechanical spectroscopy in conjunction with molecular modeling has shown that the amorphous cellulose chains have two main relaxation motions,[29] which are rotation of the pendent hydroxymethyl group (gamma relaxation) and cooperative motion of sections of the main chain (beta relaxation). Notably the former is independent of water content in the range studied here, whereas the latter is water-dependent. In the most recent work, it was shown that hydroxymethyl rotation requires some main chain motion for spatial reasons.[30] The lack of water dependence for the NMDs microviscosity found here suggests the rotation of TEMPOL is related to the hydroxymethyl group rotations. In the PMDs, it may be that the rotation has a contribution from main chain motion that is slowed when the water is removed, leaving the side chain rotation as the dominant relaxation and increasing the microviscosity.

In the context of motion in cellulose, it should also be noted that amorphous cellulose has a relatively high free volume of 2%,[31] so that in 100 g of cotton there is approximately 1.3 mL of free volume. This free volume allows the motion to occur more easily, as indicated by the low activation energies for the rotation.[32] It is estimated that there are approximately 3×10^{-3} mol kg^{-1} of pores in cotton,[13] which shows an intriguing match with the magnitude of the loading effects in Figure 6. From the above discussion, the number of PMDs may be estimated by the inflection loading when the amorphous regions are saturated with water, ~2×10^{-4} mol kg^{-1}, which equates to 7% of the total number of pores. The results show the chains in these regions have more freedom to move and be affected by water. Larger pores are more likely to show these effects as the amorphous polysaccharide chains will be longer with more space to move in. Size exclusion chromatography gives the pore distribution,[4,27] with the majority lying in the 0.5−3 nm range, and pores larger than 4 nm represent about 6% of the total in agreement with the above. The preferred PMDs correspond to 0.7% of the total number of pores and are probably the widest pores of ~8 nm, where the increased space means that even removal of the water does not stop the faster chain relaxation.

3.3. Adsorbed and Aggregated Phases. As with the mobile fraction, the spectra from the adsorbed and aggregated (loading of 1.0×10^{-2} mol kg^{-1}) radicals were simulated via the method of Freed et al.[19] A jump model (non-Brownian) was assumed for the simulations, and the same magnetic parameters were used as for the mobile fraction, except a larger intrinsic line width was taken (1.0 G along the N−O axis). Comparison of spectra at equal loading and temperature showed that the shape of the adsorbed and aggregated fraction did not change with humidity. Therefore, as the mobile fraction decreased with decreasing humidity, simulations were only conducted on the spectra acquired at 6% RH. Typical simulations are shown in Figure 8, and the parameters are given in Table 3.

The rotational correlation times lie in the range of 7−18 ns (slow motion), decrease with temperature, and are loading-dependent. At the lowest loadings, where adsorbed radicals were observed (1.6×10^{-4} to 7.4×10^{-4} mol kg^{-1}), the correlation times and the microviscosity calculated from them, eq 3, are approximately half those found at higher loadings (from 1.1×10^{-3} mol kg^{-1}), Table 3. Also, above 1.1×10^{-3} mol kg^{-1}, it was necessary to include Heisenberg spin exchange (W_{ex}) in the simulations. These two different ranges again point to the existence of microdomains of different character. From Figure 6, at 75% humidity, the switch from PMD to NMD behavior for the mobile radicals occurs between 4.0×10^{-4} and $1 \times$

10^{-3} mol kg^{-1}, matching the switch for the adsorbed radicals. However, unlike the mobile radicals, no dependence on humidity is observed, although even under the most extreme conditions measured, 6% RH and 323 K, there is still 40% of the adsorbed water on the crystallite walls present, so not all of the relevant water is removed. Thus, as water is removed from cotton, the amorphous filling of the PMD (reflected by the mobile radicals)-becomes like that of the NMD, but the walls do not alter (reflected by the adsorbed radicals). It is also noteworthy that the activation energy calculated from the temperature dependence for the adsorbed radical rotation is 5.3 kJ mol^{-1} in the PMDs, only slightly smaller than that for the mobile radicals of 8 kJ mol^{-1}. For the NMDs, the activation energy for the adsorbed radicals is higher at 7.1 kJ mol^{-1}; however, for the mobile radicals no temperature dependence could be observed, suggesting a smaller value.

Previous work[13,33] has connotated the preferred adsorption sites to narrow pores with the same width as TEMPOL. If this is the case, then in combination with the above assignment of the PMDs to wide >4 nm pores, the wide pores must be connected to the narrow pores, and the radical adsorbs into the neck of the narrow pore. This would also explain why they are preferred/occupied first, as the narrow pores would be expected to be filled first. For the NMDs, the radical simply adsorbs on the crystallite wall of the pore. An alternative possibility is that the radicals adsorb on the walls for both PMDs and NMDs, but the wide pores of the PMDs give the surface a slightly different character due to the greater freedom for the amorphous chains that are tethered to the crystallites. In either case, the adsorbed radicals could be expected to have greater rotational mobility. For example, if in a narrow pore, the radical may rotate via chain relaxation on either wall rather than just one.

The need to include spin exchange in the simulation of the NMDs may be due to three mechanisms, spin exchange between mobile and adsorbed radicals, spin exchange between adsorbed radicals, and aggregation influencing the spectra. If spin exchange occurs between mobile and adsorbed radicals, then it would lead to broadening of the spectra of both components. Spin exchange effects are observed in the line width of the mobile radicals[12,13] but occur with a much lower exchange frequency, e.g., 4×10^6 s^{-1} for 1×10^{-2} mol kg^{-1}, than those observed for the adsorbed spectra. Thus mobile/adsorbed radical spin exchange occurs but is too slow to explain the effect on the adsorbed spectra. For exchange between adsorbed−adsorbed radicals, it is important to know the average distance between the radicals. The total surface area of the crystallites is 180 m^2 g^{-1},[4] and for a loading of 1.0×10^{-2} mol kg^{-1}, if the radicals are randomly spaced, there will be an average distance of 5.5 nm between the radicals. In a static picture, this is too large for spin exchange to occur as the radicals must be approximately at the encounter distance of ∼0.7 nm ($2R$). If diffusive motion across the crystallite surface occurs, then to achieve the observed exchange frequencies it must occur with a two-dimensional rate constant of $\sim 4 \times 10^{15}$ mol^{-1} m^2 s^{-1} and move 5.5 nm in 1.5 ns. This would correspond to a three-dimensional (3D) diffusion coefficient of 7×10^{-8} m^2 s^{-1} ($D = d^2/6t$, Einstein−Smoluchowski relation for 3D motion) and equates to an effective viscosity of only 9 cP ($D = kT/6\pi\eta r$, Stokes−Einstein relation). This viscosity is too low, even allowing for differences between the solution and surface cases, especially since the surface microviscosity estimated from the rotational correlation times is 400 cP. Consequently, the effect must be due to aggregation of some of the radicals, in agreement with previous work.[13]

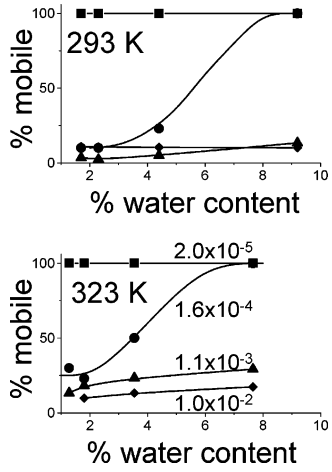

Figure 9. Variation of the mobile fraction with water content loading and temperature. The lines are guides only and have no theoretical significance.

The exchange frequency increases with temperature at both loadings, Table 3, and both gave good Arrhenius plots (not shown) with activation energies of 13 kJ mol^{-1}. This shows some motion is involved in the aggregate spin exchange, most probably a radical rotation, to bring the radical centers close enough to each other to exchange.[34] The aggregate must reduce the rotational freedom of the radicals, as the activation energy is higher than for the monomer.

3.4. Adsorption Equilibrium. *3.4.1. Quantification of the Fractions.* To quantify the fraction of adsorbed and mobile radicals, two methods could be applied, a total simulation of the spectra[12] or a simple line width and integration analysis.[13] As the latter method is simpler and quicker, it was chosen due to the large number of spectra (128) required to be analyzed. Although the reader should realize full simulation is of course possible,[35] Figure 5. The total concentration of radicals is measured from double integration of the EPR spectrum with of course a factor, α, which allows the calibration of the radical amount between the different samples. Calculation of the mobile fraction is obtained from the Lorentzian low field line width ΔH_+ and its height V_+ according to[23]

$$[\text{mobile}] = 3\alpha(1.81)V_+ \Delta H_+^2 \qquad (5)$$

The results are shown in Figure 9. For the most preferred PMDs (2×10^{-5} mol kg^{-1}), only mobile radicals are observed under all conditions, while for the PMDs (1.6×10^{-4} mol kg^{-1}) a strong increase in the number of mobile radicals is found with increasing water content, at both temperatures. These changes mirror those of the probe's microviscosity, which decreases with increasing water content, Figure 6, at this loading. For the NMDs (1.1×10^{-3} and 1.0×10^{-2} mol kg^{-1}), the mobile fraction also increases with water content but not as strongly. Again, this reflects the microviscosity results, where the NMDs were less sensitive to the water content than the PMDs.

It is intriguing that the greatest effect of water content and temperature on the radicals is to change the fraction of mobile radicals. It is probably reasonable to assume that the polysaccharide chains in the amorphous region may have similar behavior. In this case, the change in mechanical properties of cellulose with conditions[9,29] are due to changes in the fraction of amorphous polysaccharide chains that are adsorbed onto the crystallite surfaces. At higher temperature and humidity, fewer chains are adsorbed, making mechanical motion easier, as is observed.

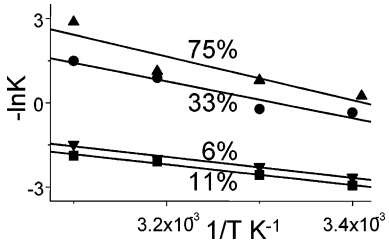

Figure 10. Plot of $-\ln K$ vs $1/T$ for a loading of 1.6×10^{-4} mol kg^{-1} and various humidities.

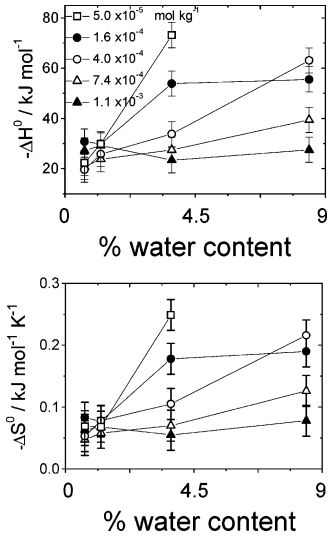

Figure 11. Loading and water content dependence of the entropy and enthalpy changes for the adsorption process.

To further quantify the changes in the mobile adsorbed fraction with water content, the spectra with no or limited aggregation were analyzed ($\leq 1.1 \times 10^{-3}$ mol kg^{-1}). Here, the adsorbed fraction is simply ([total] − [mobile]) since the aggregated fraction can be neglected at these loadings. It is reasonable to assume that an equilibrium exists between the mobile and adsorbed radicals, and this may be quantified by an experimental equilibrium constant K defined as

$$K = \frac{[\text{adsorbed}]}{[\text{mobile}]} = \frac{[\text{total}] - [\text{mobile}]}{[\text{mobile}]} \qquad (6)$$

where concentrations are all expressed in mol kg^{-1} cotton. From Table 1, the water content does not change greatly over the temperature range for each relative humidity. Hence, values for the enthalpy ΔH^0 and the entropy ΔS^0 of the adsorption process as a function of water content may be obtained from the temperature dependence of K at each RH via

$$-\ln K = -\frac{\Delta S^0}{R} + \frac{\Delta H^0}{RT} \qquad (7)$$

where R denotes the molar gas constant. Good linear plots are obtained (Figure 10), and the extracted values of ΔH^0 and ΔS^0 are plotted in Figure 11. At the lowest water content, all the microdomains where adsorbed species are observed have within error the same ΔH^0 and ΔS^0 of -25 kJ mol^{-1} and -70 J mol^{-1} K^{-1}. The enthalpy values match what would be expected for hydrogen bonds and/or dispersion forces, which typically drive adsorption processes. For simple adsorption processes, slightly smaller entropies than those that are found for evaporation would be expected, which are typically 100 J mol^{-1} K^{-1}, in good agreement.[13] Thus, at low water content, the adsorption of mobile radicals to the crystallite surface appears to be a relatively straightforward process for all the measurable pores. Above 3% water content, when absorbed water is present in the pores, the magnitude of the enthalpy and entropy increases strongly for the loadings dominated by the PMDs (5×10^{-5} and 1.6×10^{-4} mol kg^{-1}), and much less so for the loadings dominated by the NMDs (7.4×10^{-4} and 1.1×10^{-3} mol kg^{-1}). The increase in $T\Delta S°$ nearly matches the increase in $\Delta H°$, an observation that is typical in the presence of a preequilibrium. The preequilibrium is probably due to the adsorption of water on the surface of cotton, as represented in Scheme 1.At water contents below 3%, there is not full surface coverage of the crystallites by adsorbed water; hence TEMPOL (marked T in Scheme 1) may simply adsorb without the need to displace water, and so $K = K_1$ for all loadings. As would be expected, nearly all the TEMPOL adsorbs under these conditions, and from the ΔH^0 and ΔS^0 values, the desorption temperature would be 360 K.

SCHEME 1

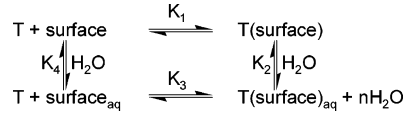

At high water contents, the crystallite surfaces are covered by adsorbed water, and it might be expected that n water molecules must be displaced for TEMPOL adsorption to occur, so that now $K = K_3$. Additionally, the mobile TEMPOL, T_{aq}, is in the presence of water. Interestingly for the NMDs the water content has very little effect on the adsorption, and thus these effects do not appear important, the equilibrium always being described by the simplest process, K_1. However, for the PMDs large effects are noted, indicating these effects are important. In this case, from Scheme 1 it is clear that

$$\Delta G_3{}^0 = -\Delta G_4{}^0 + \Delta G_1{}^0 + \Delta G_2{}^0 \qquad (8)$$

As TEMPOL is highly soluble in many solvents and shows little partition behavior even between water and octanol ($\log P = 0.6$),[36] $\Delta G^0{}_4$ will be negligible. Thus from the experimental values of enthalpy and entropy for equilibria 1 and 3, the values for water adsorption can be obtained ($-\Delta G^0{}_2/n$). If $n = 1$, then values of -36 kJ mol^{-1} and -130 J mol^{-1} K^{-1} for the enthalpy and entropy of water adsorption, respectively, are obtained. From the measured water isotherm,[8] values of -49 kJ mol^{-1} and -138 J mol^{-1} K^{-1} may be estimated for the enthalpy and entropy, respectively, in rather good agreement.

4. Conclusion

The behavior of TEMPOL in cotton may be understood in terms of two major microdomain types of different character and from the known behavior of water in cotton. In both domains, mobile radical motion is controlled by chain relaxation, and in the preferred domains, but not the most numerous, there is a small water content dependence. The mobile radical motion has a much lower activation energy than that found in liquids, which agrees with a relatively high free volume in the polymer. The adsorbed radical rotation is much more temperature-dependent, reflected by a higher activation energy. Interestingly, however, for all microdomains the biggest effect of water addition and an increase in temperature is to increase the fraction of mobile radicals.

References and Notes

(1) Betts, A.; Van Der Borg, K.; DeJong, A.; McClintock, C.; Van Strydonck, M. J. *Arch. Sci.* **1994**, *21*, 489.

(2) Pope, K. O.; Pohl, M. E. D.; Jones, J. G.; Lentz, D. L.; Von Nagy, C.; Vega, F. J.; Quitmyer, I. R. *Science* **2001**, *292*, 1370.
(3) *Cotton: World Markets and Trade*; Circular FC 05-02; U. S. Department of Agriculture.
(4) Krässig, H. A. *Cellulose*; Gordon Breach Science Publishers: 1993.
(5) Klemm, D.; Philipp, B.; Heinze, T.; Heinze, U.; Wagenknecht, W. *Comprehensive Cellulose Chemistry*; Wiley-VCH: Weinheim, 1998; Vol. 1.
(6) Wang, T. C.; Ang, T. T. *J. Phys. Chem.* **1985**, *89*, 4047.
(7) Vittadini, E.; Dickinson, L. C.; Chinachoti, P. *Carbohydr. Polym.* **2001**, *46*, 49.
(8) Jeffries, R. *J. Text. Inst.* **1960**, *51*, 339.
(9) Brown, K. C.; Mann, J. C.; Peirce, F. T. *J. Text. Inst.* **1930**, *21*, T186.
(10) Cantergiani. E.; Benczedi, D. *J. Chromatogr., A* **2002**, *969*, 103.
(11) Batchelor, S. N.; Carr, D.; Coleman, C. E.; Fairclough, L.; Jarvis, A. *Dyes Pigm.* **2003**, *59*, 269.
(12) Batchelor, S. N. *J. Phys. Chem. B* **1999**, *103*, 6700.
(13) Scheuermann, R.; Roduner, E.; Batchelor, S. N. *J. Phys. Chem. B* **2001**, *105*, 11474.
(14) *CRC Handbook of Chemistry and Physics*, 84th ed.; Lide, D. R., Ed.; CRC Press: Boca Raton, FL, 2003, pp 15−26.
(15) Knauer, B. R.; Napier, J. J. *J. Am. Chem. Soc.* **1976**, *98*, 4395.
(16) The total surface area of the crystallites of 180 m^2 g^{-1},[4] which when combined with the area per water molecule of approximately 18 $Å^2$, also gives the total surface coverage at 3% water content.
(17) Abbott, L. C.; Batchelor, S. N.; Oakes, J.; Lindsay-Smith, J. R.; Moore, J. N. *J. Phys. Chem. B* 2004, **108**, 13726.
(18) Batchelor, S. N.; Shushin, A. I. *J. Phys. Chem. B.* **2001**, *105*, 3405.
(19) (a) Schneider, D. J.; Freed, J. H. In *Spin Labeling: Theory and Applications*; Berliner, L. J., Reuben J., Eds.; Biological Magnetic Resonance 8; Plenum: New York, 1989; p 1. (b) Budil, D. E.; Lee, S.; Saxena, S.; Freed, J. H. *J. Magn. Reson., Ser. A* **1996**, *120*, 155.
(20) Hemminga, M. A.; van den Dries, I. J. In *Spin Labeling: The Next Millennium*; Berliner, L. J., Ed.; Biological Magnetic Resonance 14; Plenum: New York, 1998; p 339.
(21) Kuznetsov, A. N. *Spin Probe Technique*; Nauka: Moscow, 1976; p 53.
(22) Roozen, M. J. G. W.; Hemminga, M. A. *Spec. Publ. R. Soc. Chem.* **1991**, *82*, 531.
(23) Schreier, S.; Polnaszek, C. F.; Smith, I. C. P. *Biochim. Biophys. Acta* **1978**, *515*, 395.
(24) Batchelor, S. N.; Shushin, A. I. *Appl. Magn. Reson.* **2002**, *22*, 47.
(25) Hunt, P.; Worrall, D. R.; Wilkinson, F.; Batchelor, S. N. *J. Am. Chem. Soc.* **2002**, *124*, 8532.
(26) Edwards, J. T. *J. Chem. Educ.* **1970**, *47*, 261.
(27) Newling, B.; Batchelor, S. N. *J. Phys. Chem. B* **2003**, *107*, 12391.
(28) Yakunin, N. A.; Zavadskii, A. E.; Moryganov, A. P. *Polym. Sci. Ser. A* **2003**, *45*, 456.
(29) Montes, H.; Mazeau, K.; Cavaille, J. Y. *Macromolecules* **1997**, *30*, 6977.
(30) Einfeldt, J.; Meissner, D.; Kwasniewski. A. *Cellulose* **2004**, *11*, 137.
(31) Pekarovicova, A.; Venditti, R. A.; Cao, H.; Lou, Y. M.; Jean, Y. C. *J. Pulp Pap. Sci.* **1997**, *23*, J101.
(32) Matsuoka, S. *J. Res. Natl. Inst. Stand. Technol.* **1997**, *102*, 213.
(33) Rouquerol, F.; Rouquerol, J.; Sing, K. *Adsorption by Powders and Porous Solids: Principles, Methodology and Applications*; Academic Press: San Diego, 1999; p 113.
(34) Molin Yu. N.; Salikovm K. M.; Zamarev, K. I. *Spin Exchange*; Springer: Berlin, 1980.
(35) Ottaviani, M. F.; Turro, N. J.; Jockusch, S.; Tomalia. D. A. *J. Phys. Chem. B* **2003**, *107*, 2046.
(36) Fuchs, J.; Nitschmann, W. H.; Packer, L.; Hankovszky, O. H.; Hideg, K. *Free Radical Res. Commun.* **1990**, *10*, 315.